Available online at www.sciencedirect.com
ScienceDirect
Journal of Bionic Engineering 12 (2015) 250–262

Tendril-Based Climbing Plants to Model, Simulate and Create Bio-Inspired Robotic Systems

Renato Vidoni[1], Tanja Mimmo[1], Camilla Pandolfi[2]

1. *Faculty of Science and Technology*, *Free University of Bolzano*, *Piazza università*, 39100 *Bolzano*, *Italy*
2. *European Space Agency-Advanced Concepts Team*, *Estec*, *Noordwjik*, *Netherlands*

Abstract

Bioinspiration can be considered one of the keys for future smart and versatile robotic systems. Plants could be an important source of ideas despite the fact that they have not yet been deeply observed and considered. In this paper, climbing tendril-bearer plants that, by means of irritable filiform organs called tendrils, search for a support, grasp it and climb to gain height, have been used to study and develop an effective climbing robot. The study aimed first to evaluate the main movements and behaviors of the tendril from a biomimetic point of view. The tendril complexity was then simplified, a robotic model was developed and a kinematic simulator was designed and implemented to visualize and evaluate the chosen system. Finally, based on the biological, technical and numerical evaluations, the main tendril behaviors were replicated by proof of concept devices made of smart materials to move towards a practical realization and to replicate the simulated results. The designed proof of concept prototypes showed good repeatability and feasibility.

Keywords: climbing plants, robotic tendril, kinematic model, Shape-Memory-Alloy (SMA), grasping

doi: 10.1016/S1672-6529(14)60117-7

1 Introduction

Natural rules, concepts, mechanisms and principles can inspire new engineering technologies, algorithms, devices and solutions[1,2].

In the literature, different and successful biomimetic approaches can be found in the robotics field, in particular for mimicking legged animals, birds and insects[3–9].

Very often robotic-inspiration comes from the animal world. To date, the most effective climbing robotic systems are inspired by spiders and geckos. Indeed, on one hand, claw-systems have been realized for climbing rough hard surfaces (stone) or soft surfaces (tree bark, leaves)[10], while on the other hand, dry-adhesive systems have been designed and prototyped for climbing almost-smooth surfaces[3,8,9].

Plants can be an important source of ideas[11] even if they have not yet been deeply observed and considered. Plants climb by first winding with a consequent grasping exploiting different techniques. To give robots the grasping ability, most of the researches have focused on mechanical hands since the eighties[12,13]. Grasping hands have been studied from different biomimetic points of view: tactile sensing, restraining (fixturing) and manipulating with fingers (dexterous manipulation). To this end, both the grasping hand behavior mathematical model and the recognition of the object form and position can be considered as complex tasks. As a consequence, robotic grasping systems can usually only assume most or all the information needed for the grasping or exploit vision to obtain a relevant object's features[14,15]. Anthropomorphic multifingered grasping/fixturing can be classified in two ways: enveloping or fingertip grasp. Exhaustive reviews on these topics have been published[16–18]. Winding robotic systems have been considered and designed to replicate the capabilities of some special animals such as snakes. Hirose's group, starting from a study of snake movements[19] developed a class of rigid-link hyper redundant dexterous manipulators called "Active Cord Mechanism" (ACM) or "serpentine robots". Robinson and Davies studied a class of continuum manipulators[20], systems with a backbone structure with a high number of

Corresponding author: Renato Vidoni
E-mail: renato.vidoni@unibz.it

joints and a very short length of links. This approach leads to an ideal continuum structure that can bend, contract and extend at any point (*e.g.* Refs. [21, 22]). Today, artificial tendons and artificial muscle technologies are effective hardware realizations. Other successful works on backbone manipulators are the octopus and the arms and tentacles of squid-inspired robots[23], *e.g.* the OCTARM robot, and the trunk and tentacles-inspired robot[24,25], *e.g.* Air Octor. Recently, in the Octopus Project (EU-FP7), novel design principles and technologies for a new generation of high dexterity soft-bodied robots inspired by the morphology and behavior of the octopus have been studied[26,27]. The development of an effective climbing bio-inspired robot is still a challenge. In this work, the biomimetic approach has been applied to climbing tendril-bearer plants that, by means of tendrils, search for a support, grasp it and climb[28,29]. Tendrils are filiform, long, irritable organs, derived from stems, leaves, or flower peduncles[28] which may occur either as un-branched or multi-branched organs with a variable length, from 3.8 cm to 40 cm[30]. Besides a general sensitivity for mechanical stimuli, many plants have evolved specialized organs with highly developed mechanisms to perceive and transduce the applied forces[31]. *Mimosa pudica* L for example, responds to touch by folding up its leaflets. The stimulus then propagates from one leaflet to the adjacent one and ultimately to adjacent leaves[32]. Concerning touch-induced movements, tendrils are able to coil around a support and grasp it, enabling the plant to achieve vertical height without a proper supporting trunk. As first described by Charles Darwin, tendrils perform three main movements[28,30]:

• Circumnutation, an endogenous movement increasing the probability of contact with supports, Fig. 1;

• Contact coiling, in which the stimulated tendril coils around a support, Fig. 2a;

• Free-coiling, in which the tendril develops helical coils along its axis, not necessarily as a result of stimulation, Fig. 2b and Fig. 2c.

Circumnutation, which was first introduced by the Darwins (father and son[33]), is an oscillating growth pattern in rapidly elongating plant organs, such as roots, shoots, branches and flower stalks. Circumnutational oscillations are the manifestations of radially asymmetric growth rate, the typical of elongating plant

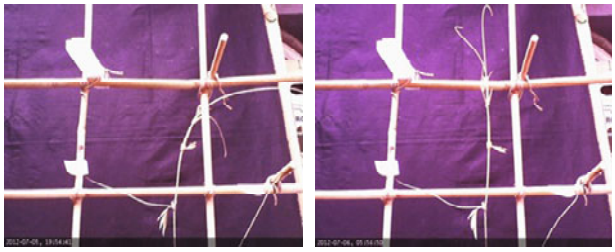

(a) (b)

Fig. 1 Tendril circumnutation behavior: by growing (a), the tendril sweeps and searches a support (b)[34].

(a) (b) (c)

Fig. 2 Tendril coiling behaviors: (a) grasping by coiling; (b) free-coiling and (c) perversion effect[34].

organs[35]. Darwin's close observation of the behavior of climbing plants led him to speculate that they exploit this movement for "searching" for an upright support. The circumnutational movement sweeps the tendril about in different paths increasing the possibility of contact with a support. Maximum tendril circumnutation usually coincides with the period of maximal sensitivity of the organ[36]. Moreover, the rotation seems related to the path of the sun and to the age of the tendril[37]. Circumnutation is a very complex and highly variable plant behavior ruled by different parameters but the mechanisms behind the circumnutation are, to date, not perfectly known. Both a deeper study on the molecular mechanism, and a better and wider description of the circumnutation parameters are needed[38].

Contact coiling, or simply coiling, initiates in response to a local mechanical stimulus of the tendrils which start curling around a support, as shown in Fig. 2, and tightening up[39]. In some species the process is reversible; indeed, if no suitable contact or support is found, the tendril might uncoil. In addition, plants are able to discriminate between stimuli; for instance, water droplets during a rain fall do not induce any coiling[40]. The tendril seems to perceive the stimulus/touch in the epidermal cells activating chemical signaling within the whole plant organ[41]. This response is very fast, leading to the start of the movement within seconds. Many authors have demonstrated that the tendril coiling is associated to the presence of gelatinous fibers, the so-called

G fibers[42]. With the decrease in the water content these fibers contract generates a contractile force and thus leads to tendril coiling.

Once the tendril has grasped around a support, the plant organ undergoes a secondary coiling, called free-coiling, which brings the plant closer to the support. This pulling movement creates an elastic spring-like connection between the stem and the grasped support, able to resist high wind and load. During the free-coiling process, the cell structure dehydrates, including the G fibers, and thus becomes more rigid, preventing an uncoiling. In general, lignification seems to be highest in the fibers closest to the touching surface[42]. This spring-spiral structure has very often been compared to a telephone cord and might be described by an ideal helical spring. Darwin *et al*.[37] observed that the same numbers of spirals are created in both directions (clockwise and counterclockwise) in order to create a zero-twist on the axis. The segment of spiral inversion, which unifies the two helices, is called tendril perversion, as shown in Fig. 2b. If no grasping occurs, the tendril curves and creates a sort of spiral.

This work addresses a different climbing method based on a grasping-by-coiling phase followed by a pulling behavior inspired by tendril-bearer plants. First, the tendril behaviors and key principles and solutions are highlighted and described in section **2**. A bio-inspired robotic tendril is then conceptualized and a simplified kinematic model is developed and simulated in section **3**. Finally, the results for a modular robotic prototype are presented and discussed in section **4**.

2 Tendril technical highlights: models and algorithms

To our knowledge, a biomimetic approach has never been applied for studying and replicating plant tendril behaviors, in particular for the coiling and free-coiling phases. Moreover, many important features and differences between plants and the well-studied behaviors of animals can be found. For instance, the circumnutation phase is the result of a sweeping movement to encounter and touch a possible element to grasp. This object searching phase can substitute, from a biomimetic point of view, complex and expensive sensors. Biologically, it is a manifestation of the radial growth of cells that results in a sweeping "seek" movement. For biomimetic purposes, it can be simplified into a movement created by a proper active joint at the tendrils base.

With regard to grasping behavior, tendrils *(e.g. Passiflora tendrils*) can recognize supports and obstacles on the overall surface by means of specialized surfaces or cells. Indeed, tendrils are able to bend in different directions. In addition, depending on the position of the touching point, tendrils can create multiple coils around the grasped element. In such a configuration, two big advantages can be detected: (1) The coils can be seen as a winch-capsant system, with a tension negligible at the apex and increasing towards the initial touching point; (2) the increased touching surface due to the multiple coils will increase the related friction, reducing the force needed to secure the hold.

If the contact reaction is analyzed, a reflex modular distributed behavior can be appreciated (see Fig. 3). Indeed, the second part of the tendril is its most sensitive part. Therefore, once a stimulus is given/recognized, a reflex behavior occurs, *i.e*. the tendril bends in the direction of the stimulus. The zone that has sensed a support induces thereby a fiber contraction and thus the bending. After that, if the contact increases, *i.e*. other near zones sense a contact, the bending signal seems to be propagated in these zones collectively, creating the overall tendril grasping and coiling. A distributed reflex control seems to be the coiling driver, allowing the activation of localized motion, only when necessary and in an energy-efficient way.

Finally, the free-coiling phase, *i.e*. the pulling that brings the stem towards the grasped support, is another feature that surely can inspire biomimetic devices and techniques. By lignifying and forming the original/intrinsic helical shape, the tendril shortens the distance between the fixed end-points and moreover, the helical-spring shape is both able to create a strong pulling force and be perfectly tuned to resist external loads and

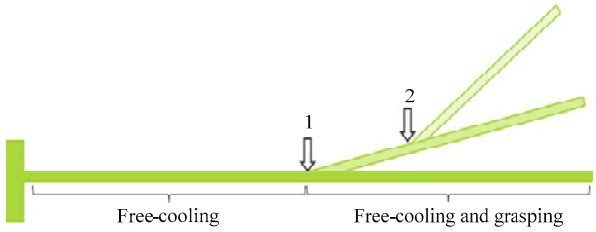

Fig. 3 Tendril reflex behavior: if the tendril hits an obstacle (1), it bends the remaining part; if the rest of the tendril encounters the obstacle the bend is propagated (2); otherwise it stops.

disturbances. The phenomenon that allows it to obtain this result, as previously stated, is called perversion[37] and the tendril passes from a linear wire condition to a spiral structure without allowing the torsion of the wire extremities, *i.e.* the fixed points in case of grasping. Moreover, it also allows the tendril to create a sufficient pulling force to move the stem towards the grasped object.

The effectiveness of the chosen solution can be better understood looking at the spring-related classical mechanical theory, *i.e.* helical springs. An ideal spring follows Hooke's law, *i.e.* $F = K\,x$, where F is the applied force, x the displacement and K the elastic constant that is related to the geometrical and physical properties of the elastic element. For the helical spring, given the coil diameter D, the number of coils n_c, the wire diameter d_t, the applied force F and the shear modulus G, the elastic constant can then be computed as[43]

$$K = \frac{G d_t^4}{8 D^3 n_c}. \tag{1}$$

Looking at Eq. (1), to decrease the helix stiffness K, the number of coils n_c has to be decreased. From another point of view, the stiffness K is inversely proportional to the coil diameter D in a cubic way; hence, the lower the diameter, the greater the stiffness. Moreover, by assuming a fixed wire length, D and n_c are not independent since the number of coils is directly related to the coil diameter. Then, by naming l_0 the tendril length of the Free-Coiling (FC), it can be written as $l_0 = n_c \pi D$. By substituting l_0 in Eq. (1), a simplified relation can be found

$$K = \frac{G d_t^4 \pi \Delta}{8 D^3 l_0} = \frac{G \pi d_t^4}{8 D^2 l_0}, \tag{2}$$

thus, the greater the coil diameter the lower the stiffness. Therefore, it is better to minimize the coil diameter in order to minimize the coil number. This explains why the free-coiling phase creates helices with a small diameter to pull up the stem of the plant. All these features strongly support the study and design of a plant-inspired robotic tendril.

3 Robotic tendril concept

This section addresses the modeling of a climbing-plant inspired robotic system with the above described features, *i.e.* support recognition, bending in different directions, grasping and eventually climbing with the use of a FC pulling.

3.1 Kinematic model

The overall structure has been firstly considered from a kinematic point of view to design a biorobotic tendril. The model has been conceptualized and simplified by defining two main parts (see Fig. 4), considering the different degree of sensitivity along the filament length:

- FC part, mainly devoted to the free-coiling and pulling phase,
- Grasping-Coiling (GC), devoted to the coiling and grasping phase.

Then, the GC part can be subdivided into independent elements that react when stimulated, and bend. The pulling FC part can be viewed as a single actuator (eventually made of multiple sections) that changes its shape from a linear wire to a helical spring.

To model the GC part, the work of Jones *et al.*[22] and Hannah *et al.*[44] on the kinematics of multi-section continuous robots has been chosen as starting point: each sub-section has been kinematically modeled and described by means of elementary pairs/joints and exploiting the Denavit-Hartenberg (DH) notation. By doing so, the reflex modular motion can be implemented and simulated. Then, the kinematics of the tendril GC part can be modeled using closed-form equations.It is divided into sections that can bend in at least two dimensions.

3.2 GC part

The GC part is considered as subdivided into n-sections. The main assumption is that the tendril section has a constant curvature. A real tendril lacks joints but each tendril section can be viewed as an arc of constant curvature, *i.e.* by means of parameters such as

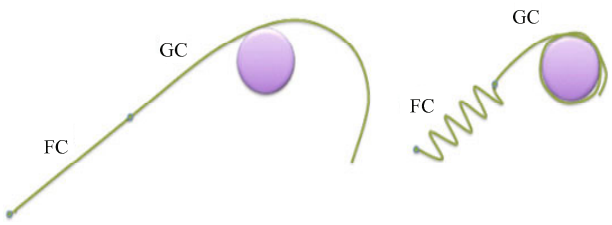

Fig. 4 GC and FC modules of the bio-mimetic tendril model.

length, curvature and/or angle of curvature. The equivalence and the relations between this kind of representation and a conventional DH formulation are obtained by designing an equivalent rigid-link-joint section.

Thus, the relationship is $[\theta, d]^{\mathrm{T}} = f(l,\kappa,\varphi)$ (Fig. 5), where θ and d are the DH parameters, l is the length section, κ is the curvature and φ is the angle of curvature. Hence, to fit a conventional rigid-link manipulator to the tendril, a simplified structure has been firstly considered from a kinematic point of view to design a biorobotic tendril. The model has been conceptualized and simplified by defining robotic system made of rigid links and joints, Fig. 6, has been defined with three main joints: a first universal joint, i.e. two revolute pairs with orthogonal and intersecting axis of rotation; a prismatic joint, and a second universal joint. The last joint and the related variables are coupled with those of the first joint of the following section. The first pair allows the rotation of the local frame axis to be oriented to the section tip; the prismatic joint allows the translation to the final coordinate frame origin; and the last pair allows for the correct rotation and orientation of the local frame in accordance with the following section, *i.e.* the last two joint variables are coupled with the first two. The independent variables result in three per section. If the number of sections is sufficiently high, the prismatic joint can be constrained, since the error made considering the distance between the two universal joints as a constant value becomes negligible. Finally, fixed rotations are added on the x-axis at the beginning of the DH table to have the section extension along the z-axis, and at the end of the DH table to correctly orient the tip. Table 1 shows the DH parameters related to a tendril section.

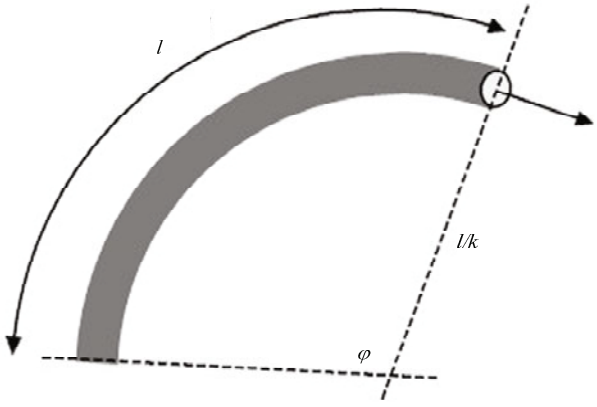

Fig. 5 Tendril section geometry and parameters[34].

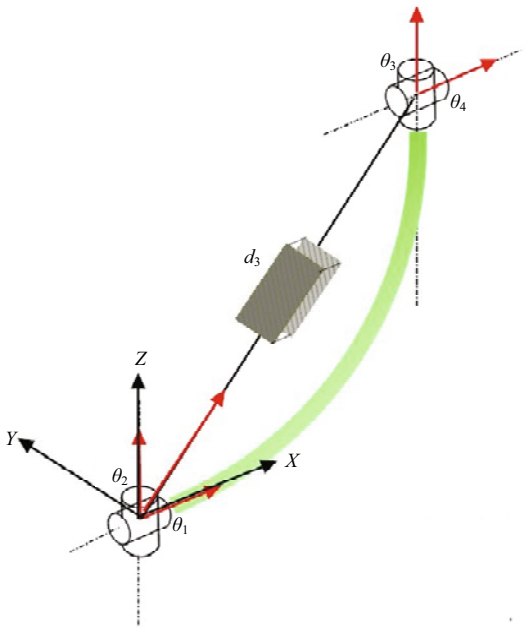

Fig. 6 Robotic section made of two universal joints and a prismatic joint associated to a tendril section (green). The red arrows represent the Z-axis of the degrees of freedom of the joints[34].

Table 1 DH tendril section parameters

Link	a	α	d	θ
-	0	$\pi/2$	0	0
1	0	$\pi/2$	0	θ_1
2	0	$\pi/2$	0	$\theta_2+\pi/2$
3	0	$-\pi/2$	d_3	0
4	0	$-\pi/2$	0	$\theta_3+\pi/2$
5	0	0	0	θ_4
–	0	$-\pi/2$	0	0

The resulting homogeneous transformation matrix for each section of the GC part is

$$\boldsymbol{A}=\begin{bmatrix} -c_1s_2s_4c_5+c_1c_2c_4c_5-s_1s_5 & c_1s_2s_4c_5+c_1c_2c_4c_5-s_1c_5 & -c_2s_4c_1+s_2c_4 & c_1c_2d_3 \\ -s_1s_2s_4c_5+s_1c_2c_4c_5-c_1s_5 & s_1s_2s_4c_5+s_1c_2c_4s_5-c_1c_5 & -s_1c_2s_4+s_2c_4 & s_1c_2d_3 \\ (c_2s_4+s_2c_4)s_5 & -(c_2s_4+s_2c_4)s_5 & c_2c_4+s_2s_4 & s_2d_3 \\ 0 & 0 & 0 & 0 \end{bmatrix}, \tag{3}$$

where $\cos(\theta_i)$ and $\sin(\theta_i)$ are compressed as c_i and s_i, respectively.

If a planar 2-D motion is considered, the tendril curve lies in a plane. If a constant curvature hypothesis is maintained, each section can be associated to a planar robotic system made of a prismatic joint between two revolute joints with axes of rotation perpendicular to the plane.

The geometrical transformation between the DH parameters and the parameterization of the tendril as a spatial curve, *i.e.* l, κ, φ, can be found by looking at the geometry of a tendril section starting from the adopted constant curvature hypothesis.

Indeed, in such a condition, each tendril section can be considered or viewed in a 2-D plane π. Its coordinates are:

$$(x, y)_\pi = (\cos(\frac{kl-1}{k}), \sin(\frac{kl}{k})), \tag{4}$$

In the rototranslation matrix $\boldsymbol{A}$, these coordinates are the translational terms $\boldsymbol{A}(1,4)$ and $\boldsymbol{A}(2,4)$ respectively. The distance d_3 between the extreme points of the tendril section can be found as:

$$d_3 = \frac{2}{k}\sin(\frac{kl}{2}), \tag{5}$$

Now, thanks to geometrical and trigonometric identities, the system can be solved and the independent variables computed as:

$$\theta_1 = \tan^{-1}\left(\frac{-1}{\tan(\frac{kl}{2})\cos(\varphi)}\right), \tag{6}$$

$$\theta_2 = \sin^{-1}\left(\sin(\frac{kl}{2})\sin(\varphi)\right), \tag{7}$$

Since the last two rotations restore the initial orientation, the final relationship result is

$$[\theta_1, \theta_2, d_3, \theta_3, \theta_4]^{\mathrm{T}} = \begin{bmatrix} \tan^{-1}\left(\frac{-1}{\tan(\frac{kl}{2})\cos(\varphi)}\right) \\ \sin^{-1}\left(\sin(\frac{kl}{2})\sin(\varphi)\right) \\ \frac{2}{k}\sin(\frac{kl}{2}) \\ \sin^{-1}\left(\sin(\frac{kl}{2})\sin(\varphi)\right) \\ \tan^{-1}\left(\frac{-1}{\tan(\frac{kl}{2})\cos(\varphi)} + \pi\right) \end{bmatrix}, \tag{8}$$

Thus, the rototranslation matrix expressed with respect to the "curve" parameters is

$$\boldsymbol{A} = \left[\begin{array}{ccc|c} \cos^2(\varphi)(\cos(kl)-1)+1 & \sin(\varphi)\cos(\varphi)(\cos(kl)-1) & -\cos(\varphi)\sin(kl) & \frac{\cos(\varphi(\cos(kl)-1))}{k} \\ \sin(\varphi)\cos(\varphi)(\cos(kl)-1) & \cos^2(\varphi)\cos(\varphi)(\cos(kl)-1) & -\sin(\varphi)\sin(kl) & \frac{\sin(\varphi(\cos(kl)-1))}{k} \\ \cos(\varphi)\sin(kl) & \sin(\varphi)\sin(kl) & \cos(kl) & \frac{\sin(kl)}{k} \\ \hline 0 & 0 & 0 & 1 \end{array}\right]. \tag{9}$$

The model, being highly flexible, can both be used to simulate the real tendril behavior by increasing the number of sections, and serve as a basis for the evaluation and control of a real modular robotic system made of independent reflexive sections. In the latter case, the robotic tendril is seen as a chain of independent embedded modules.

3.3 FC part

The FC part has been modeled by a unique kinematic section: on one side it is constrained by the stem/fixed base whereas on the other side it is constrained by the contact/grasping point. The joints of the section are the same as those previously defined, both for the 3D and 2D motions. Indeed, the first universal joint

allows the tendril to be properly oriented, the prismatic joint to consider the free-coiling main effect, and the second universal joint to take into account the correct final orientation for the connection of the two tendril parts. During grasping, the two FC part extreme points are constrained and no torsion is allowed, which means that the related angular values are defined once the grasping phase has ended. The unique joint that has to be driven for simulating the FC effect is the prismatic pai, which defines the distance between the base and the origin of the first local coordinate frame of the GC part. From the kinematic point of view, the end-effector of the section becomes the stem, and the movement has to be described with respect to the local reference frame of the last pair of the FC section, which is now constrained and fixed.

3.4 Robotic tendril simulator

Thanks to the described kinematic model, a Matlab simulator (Fig. 7) was developed for both replicating the real tendril reflex behavior and simulating a biorobotic system.

The FC part, since it is made of a unique section, is defined with a greater length with respect to the GC sections, *e.g.* half of the overall length. The FC part is constrained in position in its origin during the searching and grasping phase. On the contrary, the GC part is composed of *n* sections of equal length.

For the three main tendril behaviors the following hypothesis or simplifications are adopted:

- The circumnutation phase is reproduced with a centralized motion: only the first universal joint of the chain is driven to allow the tendril to span a cone in a 3D motion (or an angle in 2D) searching for a support to be grasped;
- The grasping phase is implemented by means of the reflex behavior previously described. For this, each GC section is an independent module. The prismatic joint is constrained in length since a large number of sections are simulated;
- The free-coiling behavior is implemented as a pulling motion driven by the prismatic joint of the FC part. In such a case, the base of the section becomes the connection point between the GC and FC parts, while the end-effector becomes the coordinate frame of the stem.

If a GC section touches an obstacle, it stops the

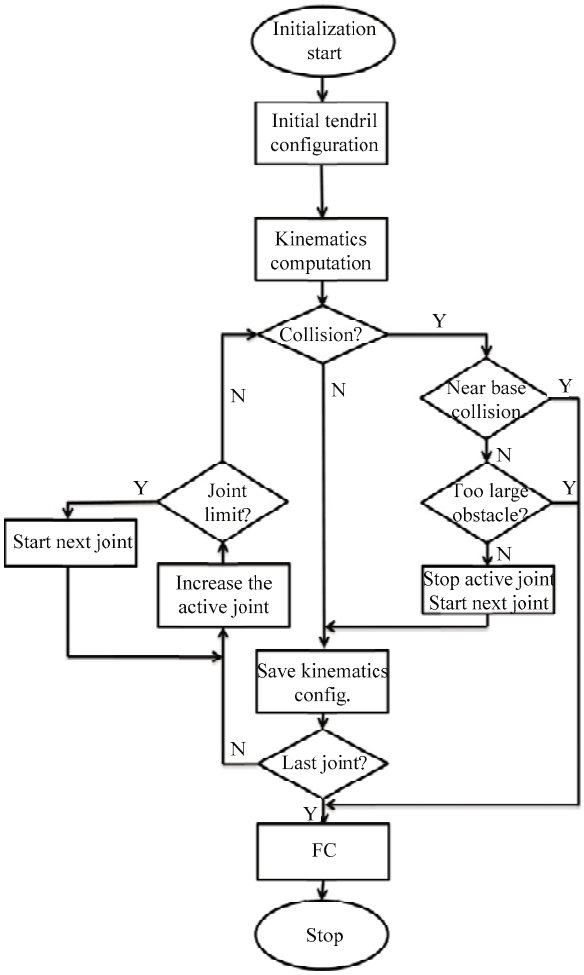

Fig. 7 Flow chart of the Matlab simulator.

main circumnutation motion. Then, the involved section reacts by bending in the direction of the stimulus. This is made by "sending an actuating signal" to the first joint of the following section, in order to bend the rest of the tendril in the stimulated direction. If another section is stimulated, *i.e.* touches the support, the bending propagation continues and the grasping by coiling goes on. On the contrary, if the minimum curvature angle is reached, the tendril motion stops and the tendril motion should be zeroed/restarted. The contact is implemented by searching for each module if there is intersection between the linear part of the section, which connects the two universal/revolute joints, and the surface to be found (for instance, a cylinder).

Two particular conditions are implemented: the minimum and maximum radius. The former is related to the intrinsic curvature of the tendril that represents the minimum radius of the object that can be coiled. The latter is related to the slippage limit, over which the

tendril slips on the surface and curls. According to the results of Goriely and Neukirch[45], the radius of the circular cross section of the support has to be smaller or equal to 3–3.5 times the tendril radius. The DH independent variables are chosen to simulate a smooth and slow motion, *i.e*. a small angular step. The shortening length in the FC phase is computed by referring to the idealized spring that has been created and by taking into account the results obtained previously, Eq. (2). Giving the spring diameter D, the number of coils n_c, and the wire diameter d_t, the linear length of the final spring is

$$l_1 = c_1 n_c d_t = c_1 \frac{l_0}{\pi D} d_t, \tag{10}$$

where l_0 is the initial free wire length and c_1 is a spring-packing coefficient that takes into account that the spring coils are not overlapped.

3.4.1 Example

In order to show the simulated results, two cases that mimic the tendril dimensions and behaviors are reported here. Table 2 shows the implemented parameters. $l_{\min}$ and $D_{\max}$ variables represent the minimum length of l_0 above which the touching would allow the coiling activity and the maximum diameter of the cylinder to be grasped over which slippage occurs, respectively.

The first case is related to a regular grasping on a cylinder with diameter 2 mm. The tendril finds the obstacle, curls and coils on it and, finally, pulls the base towards the grasping point. Fig. 8a and Fig. 8b show the circumnutation and the first hitting phase where the tendril hits the cylindrical support at about half of its length of 23 mm.

Then, Fig. 8c and Fig. 8d show the coiling phase. The tendril finds a contact of the support to grasp up to its end. It creates, in this case, four coils.

Finally, Fig. 8e and Fig. 8f show the FC phase simulated from a kinematic point of view, *i.e*. in its equivalent prismatic/linear motion, and the shortening of the free tendril part and the motion of the tendril-stem connection point.

The second case shows the simulation of a hitting and stopping when the diameter of found support is greater than the maximum allowable (Fig. 9).

The model can then serve for both replicating the tendril motion to understand its behavior, and designing a robotic system made of independent reflexive sections.

Table 2 Simulated tendril parameters

Tendril parameters	Free-coiling parameters	Obstacle parameters
Case1		Cylinder
Length = 50 mm	d_t = 1.5 mm	Radius = 1 mm
n = 100 sections	D = 5 mm	x_{position} = 10 mm
Limit angle = 60°		y_{position} = 10 mm
$l_{\min}$ = 30% of the length		
$D_{\max}$ = 17.5mm		
Case2		Cylinder
Length = 50 mm	d_t = 1.5 mm	
n = 100sections	D = 5 mm	Radius = 1 mm
Limit angle = 60°		x_{position} = 10 mm
$l_{\min}$ = 30%		
$D_{\max}$ = 17.5mm		

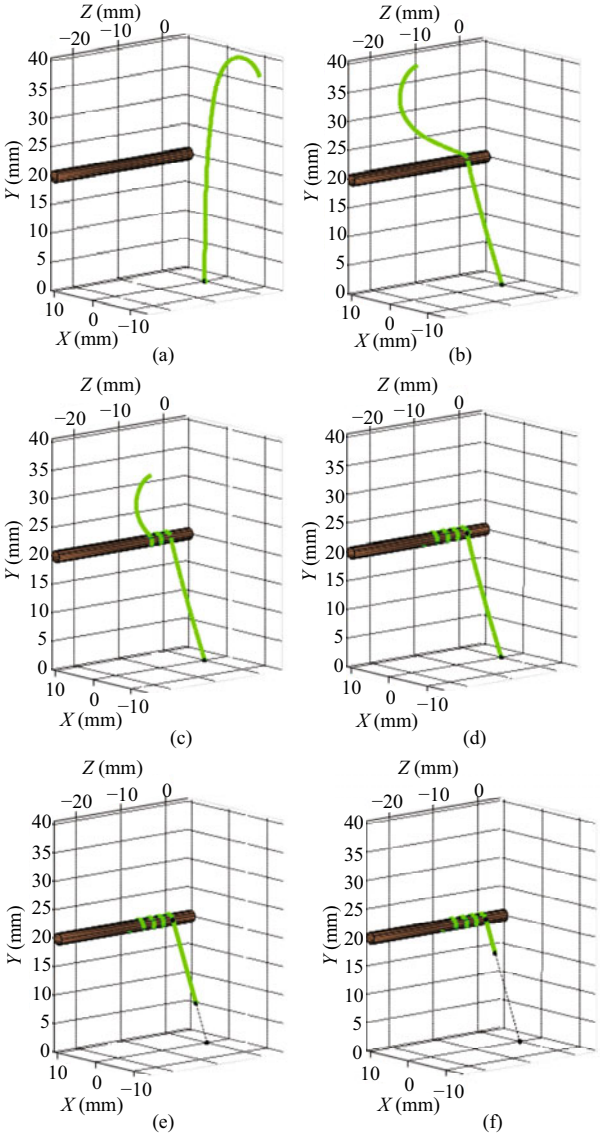

Fig. 8 Bio-mimetic tendril simulation case 1: (a) Circumnutation; (b) touching; (c) and (d) coiling/grasping; (e) and (f) FC.

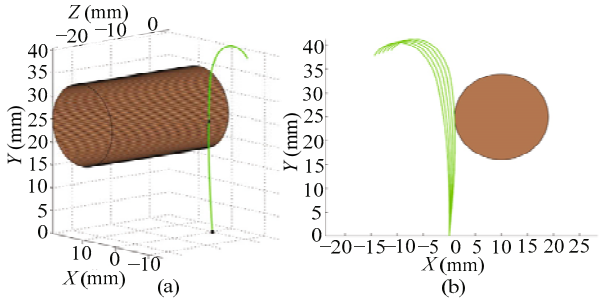

Fig. 9 Bio-mimetic tendril simulation case 2: (a) 3D view of the touching; (b) Trajectory followed by the tendril until the motion stops.

4 Towards a robotic prototype

The conceptualized GC and FC sections can be made either in a standard way by means of motorized actuators or in a light and simple system by means of wires and/or smart materials. In this context, smart materials such as Shape Memory Alloys (SMAs) can serve as technological base for developing independent actuation systems. Miniaturized touching or force sensors can serve for the contact recognition phase.

Thus, given the conceptualized system, an evaluation of a suitable solution for prototyping has been made to move towards the realization of a bioinspired robotic tendril. A GC section and the FC part replication have been focused to design and prototype proof of concept devices.

4.1 Technology for tendril-like actuators: SMA

SMAs, piezoelectric materials and electroactive polymers belong to the "intelligent materials"[46]. They can be used for substituting the classical motors by the design of smart, light and effective actuators. Indeed, such materials respond to external stimuli such as an electrical field, a magnetic field and light. The result is a shape or size modification, *i.e.* contraction, elongation, bending, *etc*. Concerning at our purpose, to reproduce and mimic tendril behavior, these can be suitable materials, especially when it is taken into account that significant applications have already been developed for biomimetic purposes[1]. Electroactive Polymers (EAP)[47], similarly to piezoelectric actuators, deform if an electric field is applied. Unlike piezo-actuators, EAPs work as biological muscles by producing strain and deflections[48].

SMAs are able to recover a predetermined shape when heated and exhibit a large energy density and a low driving voltage. In a cold condition below their transition temperature, they can be easily deformed to a generic stable shape due to the low yield strength. When the transition temperature is overcome, they return to a "memorized" shape due to the change in the crystal structure. Large forces are generated if obstacles or resistance are encountered. Two types of shape memory effects can be performed: a one-way memory effect where if no stress is applied, the material remains in the memorized shape when cooled down; a two-way memory effect where if properly trained, the material stretches back to the low temperature shape. The phase transition and the mechanical power generation driven by temperature and the Joule effect are the most common ones to cool the material even if conduction or convection is also exploited. Many robotic applications use SMAs in wire form, *e.g.* passive elastic forces or antagonistic SMA actuator pairs[49–53], creating lightweight, silent and inexpensive actuators[54].

In this work, among the possible solutions, the commercially available SMAs are chosen as basic material for a proof-of-concept realization because the slow and silent motion is not a drawback for our purposes given that the tendril motion also shows these behaviors. Indeed, the desired shape can be memorized and SMA materials can be manufactured both in wire and spring form at relatively low costs.

4.2 Proof of concepts

The biological study and the technical and technological biomimetic evaluation previously described will be exploited in this section to conceptualize a practical realization and replication of the main tendril behaviors and characteristics. Thus, the main features and movements have been prioritized and SMAs proof of concept prototypes realized in order to test the feasibility of the ideas and the approach[55].

4.2.1 Grasping by coiling

Focusing on the tendril coiling and grasping behavior, a simple and light structure able either to bend and coil or to recover a straight or almost linear shape was made through a unique element made of SMA NiTi wires. Using the wires with the length of 100 mm, a coiled or straight shape was memorized by heating them at 600 ˚C and maintaining the temperature for a couple of minutes. Thus, "coiled-if-heated" and "straight-

ened-if-heated" circuits were created. In order to control the SMA activation in a proper manner, *i.e*. by overpassing the transition temperature, a proper current has to flow through the circuit. This depends on the geometrical dimensions, the mechanical and physical properties of the material and on the velocity of actuation that is desired (Table 3). Indeed, given the wire diameter d_t = 0.5 mm, the current i required to surpass the transition temperature, *i.e*. 80 ˚C, from room temperature in about Δt = 3 s is given by the following equation

$$cm\Delta T = Ri^2\Delta t, \tag{11}$$

where ΔT is the required increase of temperature, c is the heat capacity, R is the material resistance and m is the wire mass. The computation gives a required current of about 1.3 A–1.4 A.

The straightening circuit was realized with a NiTi wire and a standard copper wire; the bending and coiling or the straightening behavior can be properly emulated by actuating the proper circuit. Fig. 10 shows the coiling and uncoiling behaviors, which were replicated many times ($n \geq 10$) showing good performance repeatability.

In a second attempt for a 2D section, NiTi springs were exploited. Fig. 11 shows that the springs act as a linear actuator and almost maintain the final configuration when cooled. The test section was made in plastic by a 3D printer and with NiTi helical springs of 29 mm in length when in the active state, and an external diameter of 6 mm. The wire diameter is 750 μm and the transition temperature is about 55 ˚C. The module is 78 mm in length and height, 24 mm in width and the pin element is at 30 mm with respect to the base. The weight of the module is about 0.08 Kg. The two helical springs are mounted in an elongated and relaxed configuration, *i.e*. plates in parallel planes, that need a spring with the length of 36 mm. By driving one of the two NiTi wires the bending motion is reached thanks to the central hinge allowing an angular displacement of about 17 deg. The hit recognition was developed by touching sensors that, if pushed, allows the contact recognition and the bending signal propagation. Indeed, a switch is put in each lateral side of the basal element. The section is driven by an external power source and, when a switch is touched, an electric circuit allows the current to flow in the proper spring. A timer was adopted both to maintain the power on in order to properly bend the module and to switch off the system to prevent energy waste, *e.g*. 2 A for 10 s. In this way, the reflex behavior together with the proper bending motion was realized with a proof of concept device.

Table 3 The physical and mechanical properties of NiTi

Property	Symbol	Value
Density	ρ	6.45 g·cm^{-3}
Resistivity (high-temperature state)	r	82 μohm·cm
Resistivity (low-temperature state)	r	76 μohm·cm
Heat capacity	c	322 J·(kg·K)$^{-1}$

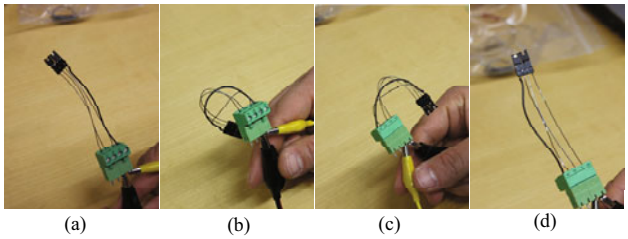

(a) (b) (c) (d)

Fig. 10 Proof of concept about coiling and uncoiling with SMA NiTi materials: (a) and (b) coiling and wrapping; (c) and (d) un-wrapping and stretching[55].

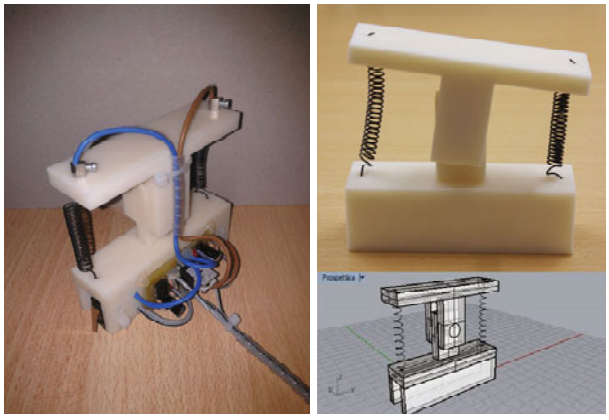

(a) (b)

Fig. 11 Proof of concept about SMA bio-tendril NiTi 2D section: Design and mechanical prototype without (a) and with (b) the electric control circuit[55].

4.2.2 FC

Focusing on the FC, we wanted to recreate the pulling with no torsion effect allowed by the spring contraction and the perversion, *i.e*. the interconnection between two helical springs with opposite twist, avoiding the use of contracting straight wires due to their poor performance. A SMA NiTi spring-like structure would allow for a good resistance to external forces, large forces and contraction. Moreover, the helical spring mechano-elastic capabilities contribute in the pulling phase. Therefore, the helical spring considerations made

in the previous sections are still valid. By memorizing a shape made of two helical springs with opposite rotation direction connected by a perversion in a NiTi element, the tendril pulling behavior can be replicated. If the end-points are constrained and current is allowed to flow in the material and provided that the memorized shape mimics the tendril, the memorized shape is recovered together with a pulling phase without torsion, as shown in Fig. 12. In an optimized future realization, the considerations on the coil diameter and helix stiffness will be exploited for tuning and realizing a proper behaviour of spring. Here, the NiTi wire is 200 mm in length and 1 mm in diameter, the transition temperature is about 80 ˚C – 90 ˚C and the applied current is set to 2.5 A to reach the transition phase in few seconds. With such a device, the relative displacement between the straight and contracted configurations is about 100 mm.

(a) (b)

Fig. 12 Proof of concept about SMA bio-tendril FC pulling phase[55]: (a) Starting; (b) final configuration.

5 Conclusion

The work reported here is a part of an ongoing study focused on the design and development of a new robotic tendril-based grasping system. A biomimetic approach has been firstly adopted to investigate and understand the capabilities and the main behaviors of tendril-based grasping plants. Then, after having identified and highlighted possible technical solutions, the tendril has been modeled from a kinematic point of view in a section-like system by dividing it into two main parts. Based on this, a Matlab simulator has been designed and the circumnutation, coiling by grasping, touch recognition, reflex reaction, and pulling by FC behaviors implemented and simulated. After that, to move towards a practical realization and to replicate the simulated results, SMA materials have been exploited due to their capabilities to recover a pre-memorized shape if heated with the production of large forces. The bending and the free-coiling motion together with the reflex behavior have been replicated with the design of proof of concept prototypes showing a good repeatability and feasibility. Current work covers the evaluation of the grasping and pulling forces achievable with the SMA materials and with the developed modules. Future work will cover the bio-inspired tendril practical realization and its control design based on the numerical results and directives obtained from the developed simulator.

Acknowledgment

This work was supported by the European Space Agency-Ariadna study (ID:12-6402).

References

[1] Bar-Cohen Y. *Biomimetics Nature-Based Innovation*, CRC press, Taylor and Francis 20 Group, 2012.

[2] Lepora N F, Verschure P, Prescott T J. The state of the art in biomimetics. *Bioinspiration and Biomimimetics*, 2013, **8**, 013001.

[3] Kim S, Spenko M, Trujillo M, Heyneman B, Santos D, Cutkosky M R. Smooth vertical surface climbing with directional adhesion. *IEEE Transactions on Robotics*, 2008, **24**, 6574.

[4] Laschi C, Mazzolai B, Cianchetti M, Margheri L, Follador M, Dario P. A soft robot arm inspired by the octopus. *Advanced Rsobotics*, 2011, **26**, 709–726.

[5] Mazzolai B, Margheri L, Cianchetti M, Dario P, Laschi C. Soft-robotic arm inspired by the octopus: II. From artificial requirements to innovative technological solutions. *Bioinspiration and Biomimimetics*, 2012, **7**, 025005.

[6] Sreetharan P, Whitney J P, Strauss M, Wood R J. Monolithic fabrication of millimeter-scale machines. *Journal of Micromechanics and Microengineering*, 2012, **22**, 05502.

[7] Vidoni R, Gaspa retto A. Efficient force distribution and leg posture for a bio-inspired spider robot. *Robotics and Autonomous Systems*, 2011, **59**, 142–150.

[8] Li Y, Ahmed A, Sameoto D, Menon C. Abigaille II: Toward the development of a spider-inspired climbing robot. *Robotica*, 2012, **30**, 79–89.

[9] Seidl T, Vidoni R. *Spider Ecophysiology*: *Adhesion to Flat Surfaces*: *From Spiders to Stickers*, In: Nentwig W (ed), Springer Berlin Heidelberg, New York, USA, 2013, 463–473.

[10] Boston Dynamics, [2013-09], http://www.bostondynamics.com/robot rise.html

[11] Mazzolai B, Mancuso S. Smart solutions from the plant kingdom. *Bioinspiration and Biomimimetics*, 2013, **8**,

020301.

[12] Siciliano B, Khatib O. *Springer Handbook of Robotics*, Springer, Berlin, Germany, 2008.

[13] Salisbury J K. *Kinematic and Force Analysis of Articulated Hands*, PhD thesis, Stanford University, Stanford, USA, 1982.

[14] Takahashi T, Tsuboi T, Kishida T, Kawanami Y, Shimizu S, Iribe M, Fukushima T, Fujita M. Adaptive grasping by multi fingered hand with tactile sensor based on robust force and position control. *Proceedings of the IEEE International Conference on Robotics and Automation*, Pasadena, CA, USA, 2008.

[15] Cannata G, Maggiali M. An embedded tactile and force sensor for robotic manipulation and grasping. *Proceedings of the 5th IEEE-RAS International Conference Humanoid Robots*, Tsukuba, Japan, 2005, 80–85.

[16] Bicchi A, Kumar V. Robotic grasping and contact: A review. *Proceedings of IEEE International Conference on Robotics and Automation*, San Francisco, CA, USA, 2000, **1**, 348–353.

[17] Tegin T, Wikander J. Tactile sensing in intelligent robotic manipulation-A review. *Industrial Robot*: *An International Journal*, 2005, **32**, 64–70.

[18] Yousef H, Boukallel M, Althoefer K. Tactile sensing for dexterous in-hand manipulation in robotics-A review. *Sensors and Actuators A*, 2011, **167**, 171–187.

[19] Hirose S. *Biologically Inspired Robots*, Oxford University Press, Oxford, England, 1993.

[20] Robinson G, Davies J B C. Continuum robots-A state of the art. *Proceedings of the IEEE International Conference on Robotics and Automation*, Detroit, USA, 1999, 2849–2854.

[21] Buckingham R. Snake arm robots. *Industrial Robot International Journal*, 2002, **29**, 242–245.

[22] Jones B A, Walker I D. Kinematics for Multisection Continuum Robots. *IEEE Transaction on Robotics*, 2006, **22**, 43–45.

[23] Walker I, Dawson D, Flash T, Grasso F, Hanlon R, Hochner B, Kier W, Pagano M, Rahn C, Zhang Q. Continuum robot arms inspired by cephalopods. *Proceedings of SPIE*, 2005, **5804**, 303–314.

[24] Jones B A, Walker I D. Practical kinematics for real-time implementation of continuum robots. *IEEE Transaction on Robotics*, 2006, **22**, 1087–1099.

[25] Walker I, Carreras C, McDonnell R, Grimes G. Extension versus bending for continuum robots. *International Journal of Advanced Robotics Systems*, 2006, **3**, 171–178.

[26] EU Octopus FP7 project, [2013-09], http://www.octopus-project.eu/

[27] Kang R, Branson D T, Guglielmino E, Caldwell D G. Dynamic model and control of a multiple continuum arm robot inspired by octopus. *Computers and Mathematics with Applications*, 2012, **64**, 1004–1016.

[28] Darwin C. *On The Movements and Habits of Climbing Plants*, John Murray, London, England, 1865.

[29] Isnard S, Silk W. Moving with climbing plants from Charles Darwin's time into the 21st century. *Journal of Botany*, 2009, **96**, 1205–1221.

[30] Jaffe M J, Galston A W. The physiology of tendrils. Annual Review of Plant Physiology, 1968, **19**, 417–434.

[31] Engelberth J. Mechanosensing and signal transduction in tendrils. *Advanced Space Research*, 2003, **32**, 1611–1619.

[32] Scorza L C, Dornelas M C. Plants on the move: Toward common mechanisms governing mechanically-induced plant movements. *Plant Signaling and Behavior*, 2011, **6**, 1979–198 6.

[33] Darwin C, Darwin F. *The Power of Movements in Plants*, Appleton, New York, USA, 1880.

[34] Vidoni R, Mimmo T, Pandolfi C. *Mimicking the Thigmotropic Behaviour of Climbing Plants to Design a Tactile-based Grasping Device for the Space Environment*. ESA-Advanced Concepts Team (ACT), Ariadna study n 12-6402, official report, 2013.

[35] Mugnai S, Azzarello E, Masi E, Pandolfi C, Mancuso S. Nutation in Plants, In: Mancuso S and Shabala S (eds). *Rhythms in Plants*: *Phenomenology*, *Mechanisms and Adaptative Significance*, Springer, Berlin, Germany, 2007.

[36] Von Sachs J. *Lectures on the Physiology of Plants*, Clarendon Press, Oxford, England, 1888.

[37] Darwin C. *The Movements and Habits of Climbing Plants*, Appleton, New York, USA, 1876.

[38] Stolarz M. Circumnutation as a visible plant action and reaction. *Plant Signaling & Behavior*, 2009, **4**, 380–387.

[39] Vaughn K C, Bowling A J. Biology and physiology of vines, In: Janick J (ed). *Horticultural Reviews*, Wiley-Blackwell, New Jersey, USA, 2011.

[40] Jaffe M J, Galston A W. Physiological studies on pea tendrils. V membrane changes and water movement associated with contact coiling. *Plant Physiol*, 1968, **43**,537–542.

[41] Liss H, Weiler E W. Ion-translo cating atpases in tendrils of bryonia-dioica jacq. *Planta*, 1994, **194**, 169–180.

[42] Bowling A J, Vaughn K C. Gelatinous fibers are widespread in coiling tendrils and twining plants. *American Journal of Botany*, 2009, **96**, 719–727.

[43] Budynas R, Nisbett K. *Shigley's Mechanical Engineering Design*, Mc Graw Hill, USA, 2010.

[44] Hannan M W, Walker I D. Kinematics and the implementa-

tion of an elephant's trunk manipulator and other continuum style robots. *Journal of Robotic Systems*, 2003, **20**, 45–63.

[45] Neukirch S, Goriely A. Twining plants: How stick should their supports be? *Proceedings of the 5th Plant Biomechanics Conference*, Stockholm, Sweden, Europe, 2006.

[46] Zrinyi M. Intelligent polymer gels controlled by magnetic fields. *Colloid* & *Polymer Science*, 2000, **278**, 98–103.

[47] Kim K J, Tadokoro S (eds). *Elecroactive Polymers for Robotic Applications*: *Artificial Muscles and Sensors*, Springer, London, England, 2007.

[48] Artificial Muscle incorporated, [2013-09], http://www.artificialmuscle.com

[49] Hartl D J, Lagoudas D C. Characterization and 3-D modeling of Ni60Ti SMA for actuation of a variable geometry jet engine chevron. *Proceedings of SPIE*, *Sensors and Smart Structures Technologies for Civil*, *Mechanical*, *and Aerospace Systems*, 2007.

[50] Lan C C, Yang Y N. A computational design method for a shape memory alloy wire actuated compliant finger. *ASME Journal of Mechanical Design*, 2009, **131**, 021009.

[51] Kyung J H, Ko B G, Ha Y H, Chung G J. Design of a microgripper for micromanipulation of microcomponents using SMA wires and flexible hinges. *Sensors and Actuators A*, 200 8, **141**, 144–150.

[52] Sreekumar M, Nag arajan T, Singaperumal M. Experimental investigations of the large deflection capabilities of a compliant parallel mechanism actuated by shape memory alloy wires. *Smart Materials and Structures*, 2008, **17**, 065025.

[53] Lan C C, Wang J H, Fan C H. Optimal design of rotary manipulators using shape memory alloy wire actuated flexures. *Sensors and Actuators A*, 2009, **153**, 258–266.

[54] Kohl M. *Shape Memory Microactuators*, Springer-Verlag Berlin Heidelberg, New York, USA, 2004.

[55] Vidoni R, Mimmo T, Pandolfi C, Valentinuzzi F, Cesco S. SMA bio-robotic mimesis of tendril-based climbing plants: First results. *Proceedings of the* 16*th International Conference on Advanced Robotics-ICAR*, Montevideo, Uruguay, 2013.